MODELING ELASTIC PROPERTIES OF RANDOMLY ORIENTED FIBER COMPOSITES

H. Moussaddy[1], D. Therriault[1], M. Lévesque[1]*
1 Laboratory for Multiscale Mechanics, Center for applied research on polymers (CREPEC),
École Polytechnique de Montreal, Montreal (QC), Canada
* Corresponding author (martin.levesque@polymtl.ca)

Keywords: *fiber composites, random orientation, elastic properties, finite element.*

1 Introduction

Randomly Oriented Fiber Reinforced Composites (ROFRC) are omnipresent in structural materials [1, 2]. They have the advantage of easy manufacturing and good mechanical properties. They are used in automotive [1, 2], aerospace [3], construction and biomedical applications. The difficulty in fully exploiting ROFRCs lies partially in the lack of modeling efforts to understand and accurately predict their properties. The objective of this work is to provide very accurate estimates for the mechanical properties of randomly oriented fiber reinforced composites. In the literature, ROFRCs modeling is usually performed either through analytical models (e.g., Mori-Tanaka [4]), or through finite element (FE) models [5]. Most FE studies of ROFRCs did not establish if the volume of material they represented is actually the Representative Volume Element (RVE) of the real material due to the complexity of the RVE determination process. As a result, one could question the validity of a wide range of published papers on the topic. Analytical homogenization schemes, like the self-consistent and that of Mori and Tanaka, can provide firsthand effective properties estimations. However, their accuracy for randomly distributed high aspect ratio fibers has never been rigorously established.

Several works have thoroughly assessed the modeling methods of simpler microstructures such as randomly dispersed spheres [6, 7] or aligned fibers composites [8]. In contrast, very few studies targeted the complex case of ROFRCs, especially for high aspect ratios (length over diameter). The highest aspect ratio for which the RVE has been reported is only of 5 [9], whereas ROFRCs materials such as carbon nanotube reinforced nanocomposites can have aspect ratios up to 1000.

The specific objectives of this work are to i) rigorously and thoroughly determine the appropriate RVE for ROFCs and ii) also evaluate the accuracy of analytical homogenization models.

In the following, the present work is described in three different sections: Sections 2 and 3 present the analytical and FE homogenization methods, respectively. Section 4 presents the RVE determination methodology. The effective properties of numerical homogenization of the RVE are compared to the analytical estimations in Section 5 in order to validate the analytical models and identify the best suited analytical method for randomly oriented fibers microstructures. The conclusions are listed in Section 6.

2 Analytical homogenization

The analytical models are categorized as one- and two-step models. In one-step models, the overall properties of ROFRCs are calculated in a single homogenization step whereas a combination of two models are sequentially used in the second approach [10]. Two-step methods are noted herein by "1st method/2nd method". Three analytical models are herein presented, namely: the one-step Mori-Tanaka (M-T) scheme, the two-step Self-Consistent (SC)/Voigt and Lielens (Li)/Voigt models.

2.1 One-step Mori-Tanaka

Benveniste [11] presented the Mori-Tanaka formulation to describe composites with randomly oriented inclusions. The stiffness tensor is evaluated using the orientational average as:

$$\mathbf{C}_{\alpha}^{\mathrm{MT}}=\mathbf{C}_{\mathrm{m}}+c_{\mathrm{f}}\{(\mathbf{C}_{\mathrm{f}}-\mathbf{C}_{\mathrm{m}}):\mathbf{T}\}:[c_{\mathrm{m}}\,\mathbf{I}+c_{\mathrm{f}}\,\{\mathbf{T}\}]^{-1} \quad (1)$$

where $\mathbf{C}$ and c denote the stiffness tensor and the volume fraction, respectively. Subscripts 'm' and 'f' represent the matrix and fiber, respectively, and curly brackets {.} stand for orientation averaging. Tensor $\mathbf{T}$ is given by:

$$\mathbf{T}=[\mathbf{I}+\mathbf{S}_{\mathrm{m}}:\mathbf{C}_{\mathrm{m}}^{-1}:(\mathbf{C}_{\mathrm{f}}-\mathbf{C}_{\mathrm{m}})]^{-1} \quad (2)$$

where $\mathbf{S}_m$ is Eshelby's tensor [12] where the matrix is the infinite media.

2.2 Two-step methods

In two-step methods, the RVE is decomposed into a number of discrete subregions α (α= 1, 2, … *n*) where the fibers are aligned along an arbitrary direction as illustrated in Fig.2. The homogenized elastic tensor of each subregion, $\mathbf{C}_\alpha$, is calculated in a first step using either of the SC scheme or Li model.

The SC scheme for aligned reinforcements is given by:

$$\mathbf{C}^{SC}=\mathbf{C}_m+c_f[(\mathbf{C}_f-\mathbf{C}_m)]:[\mathbf{I}+\mathbf{S}^{SC}:(\mathbf{C}^{SC})^{-1}:(\mathbf{C}_f-\mathbf{C}^{SC})] \quad (3)$$

where $\mathbf{S}^{SC}$ is Eshelby's tensor where the effective composite is the infinite media.

The Li model is expressed by:

$$\mathbf{C}^{Li}=\mathbf{C}_m+c_f[(\mathbf{C}_f-\mathbf{C}_m)]:[\hat{\mathbf{A}}^{Li}[(1-c_f)\mathbf{I}+c_f\hat{\mathbf{A}}^{Li}]^{-1} \quad (4)$$

where

$$\hat{\mathbf{A}}^{Li}=\{(1-c^*)[\hat{\mathbf{A}}^{lower}]^{-1}+c^*[\hat{\mathbf{A}}^{upper}]^{-1}\}^{-1} \quad (5)$$

and c^* is related to the reinforcements volume fraction as:

$$c^*=(c_f+c_f^2)/2 \quad (6)$$

$\hat{\mathbf{A}}^{lower}$ and $\hat{\mathbf{A}}^{upper}$ are given by:

$$\hat{\mathbf{A}}^{lower}=\mathbf{T} \quad (7)$$

$$\hat{\mathbf{A}}^{upper}=[\mathbf{I}+\mathbf{S}_f:\mathbf{C}_f^{-1}:(\mathbf{C}_m-\mathbf{C}_f)]^{-1} \quad (8)$$

where $\mathbf{S}_f$ is Eshelby's tensor where the reinforcement is the infinite media.

Homogenization over all subregions is performed in a second step using the Voigt model:

$$\mathbf{C}^{Voigt}=\sum_{\alpha=1..n}\mathbf{C}_\alpha V_\alpha / V \quad (9)$$

where V and V_α are the volume of composite and the volume of each subregion, respectively, and $\mathbf{C}_\alpha$ is the effective elastic tensor of a subregion calculated using one of the SC or Li models.

3. Numerical homogenization

Four steps were needed in order to compute the apparent properties of a single random microstructure: 1. random microstructure generation; 2. volume meshing; 3. enforcement of boundary conditions and; 4. computation of the apparent properties.

3.1 Microstructure generation

Fibers were assumed to be cylinders of circular cross-section. A random fiber generator in a periodic cubic cell was developed with MATLAB. The generation algorithm was based on the modified RSA scheme proposed by [13]. The generated volumes were periodic, i.e., every fiber that crossed a surface of the cubic cell penetrated back from the opposite surface. The method consisted of sequentially adding fibers into a volume, while checking for contact interferences with all previously generated fibers, until the target volume fraction was reached. When verifying fiber interferences, a minimum distance of 2.5 times the radius was imposed between two fiber axes in order to adequately mesh the space between them. If a newly added fiber interfered with another fiber, the position of the new fiber was translated just enough to respect the inter-fiber distance limit [13]. If the translation resulted in interferences with other fibers, the new fiber was removed and repositioned randomly in the same volume. This operation was repeated until the new fiber location was free from interferences. Figure 3.a) shows a periodic volume generated with the developed MATLAB script containing 10 fibers of aspect ratio 20 at 5% volume fraction.

3.2 Meshing

The generated microstructures were transferred to ANSYS FE package for meshing. In order to apply periodic boundary conditions (PBC), homologous nodes on opposite surfaces had to match each other perfectly. The external surfaces of the cubic volume located at x=0, y=0 and z=0 were first meshed using triangular surface (2D) elements, and the meshing was copied to the homologous surfaces using the “MSHCOPY” command. Afterwards, the volumes of all fibers and matrix were meshed with 10 nodes tetrahedron elements. A mesh size convergence study was conducted and is not presented in this paper for brevity. Meshing the fibers with tetrahedron elements with a maximum

edge length equivalent to the fiber radius and that of the matrix with an edge length of 1/10 of the RVE cube's edge length were required. ANSYS Parametric Design Language (APDL) was used in scripts to automate the meshing process. Figure 3.b) shows a periodic volume meshed with 10 fibers having an aspect ratio of 20 and a volume fraction of 5%.

3.3 Periodic boundary conditions

All FE models were transferred to ABAQUS/Standard FE package and solved under PBCs. In order to impose PBCs, each surface node displacement was coupled to its mirror node on the opposite surface according to:

$$\mathbf{u}_{x2} - \mathbf{u}_{x1} = \mathbf{E}\,(\mathbf{x}_2 - \mathbf{x}_1) \tag{10}$$

where $\mathbf{u}_{xi}$ is the displacement vector of the node located at $\mathbf{x}_i$, $\mathbf{x}_1$ and $\mathbf{x}_2$ are two homologous nodes on opposite surfaces and $\mathbf{E}$ is the applied strain. Readers are referred to [13, 14] for a more detailed description on the PBCs application methodology. Once the PBCs were applied, the FE models were solved in ABAQUS Standard v. 6.10 using the iterative solver option, parallelising on 3 to 10 XEON X7550 cores and using from 30 Gb to 600 Gb RAM memory per model.

4 RVE determination

The RVE is defined herein following the work of [15] as an ensemble of random finite volumes (i.e., realizations) of the microstructure that yield, in average, the effective properties of the composite. The RVE is described using two parameters: the number of realizations and the volume size (i.e., the number of fibers included in the volume element of each realization). The determination of the RVE parameters was performed according to two RVE determination criteria, one for each parameter. Several RVE criteria have been tested in [13] and assessed with respect to their estimation of composite effective elastic properties. In [13], a new RVE definition was provided in which the confidence criterion was applied for determining the number of realizations, whereas an averaging variation criterion was applied to determine the number of fibers included in the volume, as described below.

The confidence criterion is expressed by:

$$\frac{CI^{95\%}}{2\bar{Z}} \leq \epsilon \tag{11}$$

where Z refers to the targeted property being either the bulk k or shear G modulus, ϵ is a fixed tolerance, $CI^{95\%}$ and $\bar{Z}$ represent the 95% confidence interval and the arithmetic mean of the apparent moduli over the r realizations of the ensemble, respectively.

The averaging criterion [13] consists of computing the average properties of the ensemble of realizations using the arithmetic and harmonic means:

$$\bar{\mathbf{C}} = \frac{1}{r}\sum_{i=1}^{r} \breve{\mathbf{C}}_i \tag{12}$$

$$\underline{\mathbf{C}} = \left(\frac{1}{r}\sum_{i=1}^{r} \breve{\mathbf{C}}_i^{-1}\right)^{-1} \tag{13}$$

The corresponding elastic moduli denoted by $\bar{Z}$ and $\underline{Z}$ are computed from $\bar{\mathbf{C}}$ and $\underline{\mathbf{C}}$, respectively, using isotropy projectors. The estimation of the overall properties of the ensemble of realizations was considered as the average of both means:

$$\hat{Z} = \frac{(\bar{Z} + \underline{Z})}{2} \tag{14}$$

The criterion states that the RVE is obtained when the difference between the ensemble overall properties and any of both means $\bar{Z}$ and $\underline{Z}$ is within the prescribed tolerance:

$$\frac{|\hat{Z} - \bar{Z}|}{\hat{Z}} = \frac{|\hat{Z} - \underline{Z}|}{\hat{Z}} \leq \epsilon \tag{13}$$

5 Results and discussion

The elastic properties of ROFRCs have been evaluated for a wide range of fibers aspect ratios, volume fractions and contrast of properties. More than 2500 microstructures were generated, meshed and computed in order to determine RVEs and their corresponding accurate effective properties. Whenever the FE results are given, the corresponding RVE criteria tolerance ϵ is jointly specified. In this work, the contrast of properties indicates the ratio of the elastic moduli of the fibers with respect to that of the matrix.

5.1 Aspect ratio study

Figure 4 presents the effective elastic moduli of ROFRCs at 2\% volume fraction as a function of the fibers aspect ratio for a contrast of 300. All results have been normalized with respect to the matrix properties. The FE curves stop at the highest aspect ratio that was technically achievable with the modified RSA method and the available computational resources. The apparent scattering in the FE results is due to the non-zero RVE determination tolerance.

Figure 4 shows that the one-step M-T and two-step Li/Voigt analytical models provide the best bulk modulus predictions. However, for aspect ratios higher than 90, the few FE results presented in Figure 4 show very little changes in the bulk modulus when increasing the fibers aspect ratios. The analytical models do not have the same change in slope and, consequently, none of the models delivers accurate predictions for fibers aspect ratios over 100. The same conclusions were drawn for the shear modulus and for a volume fraction of 5%, but are not shown for brevity.

The fibers aspect ratio at which stiffening saturation is observed (around 100) is of major importance to numerical modeling. A similar aspect ratio saturation limit (approximately 90) was shown in the study of Tucker III and Liang [8] for the axial Young modulus of aligned fiber composites at 20% volume fraction. The aspect ratio saturation limit provides a practical venue for an accurate reproduction of the effective properties of very high aspect ratio fiber composites via the modeling of the composite with the fibers at the aspect ratio saturation limit. The saturation aspect ratio can hence be accurately used for the modeling of composites with higher aspect ratios (e.g. carbon nanotubes with an aspect ratio of approximately 1000), which are currently impossible to solve due to computational limits.

5.2 Volume fraction study

Figure 5 presents the effective elastic properties of ROFRCs for fibers of aspect ratio 10 as a function of the fibers volume fraction for a contrast of 300. For low volume fractions (up to 5%), all analytical models provide accurate estimates for the bulk shear modulus. For higher volume fractions, the model of Li/Voigt produces the most accurate bulk modulus predictions for all three aspect ratios and shear modulus predictions for aspect ratios of 10 and 20. The SC/Voigt model overestimates the effective bulk modulus of ROFRCs.

5.3 Properties contrast study

Figure 6 presents the effective elastic properties of 5% volume fraction ROFRCs for fibers aspect ratio of 20 as a function of the fibers/matrix contrast of elastic moduli. The models of M-T and Li/Voigt provide the most accurate estimates for the bulk modulus for all contrasts of properties under study. This observation can be extrapolated to higher contrasts ratios since the FE results, as well as the models of M-T, M-T/Voigt and Li/Voigt, have practically reached the properties contrast saturation limit.

6 Conclusion

The analytical models predictions of the elastic properties of ROFRCs were compared to accurate effective properties determined using FE numerical homogenization of the appropriate RVE. The comparisons were performed for a wide range of aspect ratios (up to 120), properties contrast (up to 300) and volume fractions only up to 20%.

The main conclusions are:

- The analytical models of M-T and Li/Voigt provide accurate estimations of the bulk and shear moduli of low volume fraction (up to 5%) ROFRCs and up to an aspect ratio of 90, which was found to be the aspect ratio saturation limit.
- For higher aspect ratios (over 90), tested analytical homogenization did not deliver accurate effective properties. The effective properties should be determined using numerical homogenization of the RVE using the aspect ratio saturation limit.
- The model of Li/Voigt provides the best suited model for bulk modulus predictions for volume fractions over 5%.

Therefore, it is concluded that if a single model was to be chosen for predicting the effective elastic properties of ROFRCs, the two-step method of Li/Voigt provides most accurate estimations over the largest range of microstructure parameters.

Future studies should focus on improving the numerical homogenization process for ROFRCs to extend the range of computable microstructures in order to reach higher volumes fractions and aspect ratios. In parallel, efforts

should be employed to develop analytical models that are best suited for ROFRCs with very high aspect ratios and volume fractions of fibers.

Acknowlegments

The work of Hadi Moussaddy was funded by the National Science and Engineering research Council of Canada (NSERC). Most of the computations were performed on supercomputers financed by the Canadian Foundation for Innovation (CFI) and the NSERC. These computers are hosted by the Fluid Dynamics Laboratory (LADYF) of Ecole Polytechnique de Montreal.

Figures

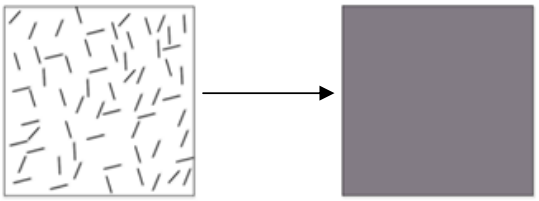

Fig. 1 One step homogenization.

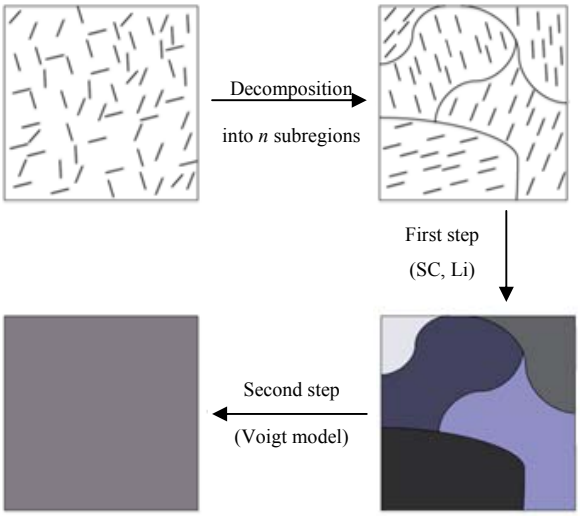

Fig.2. Two-step homogenization methods.

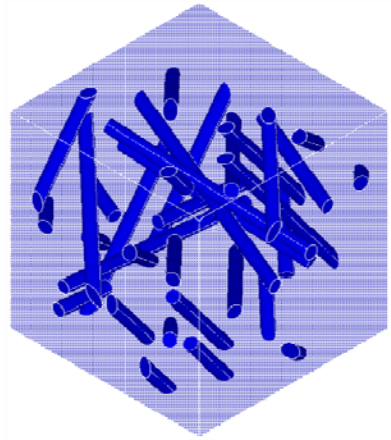

(a)

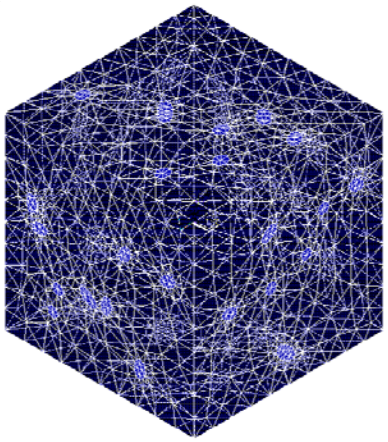

(b)

Fig.3. Generated microstructure of a ROFRC containing 10 fibers of aspect ratio 20 at 5% volume fraction. a) Periodic geometric model and b) FE meshing.

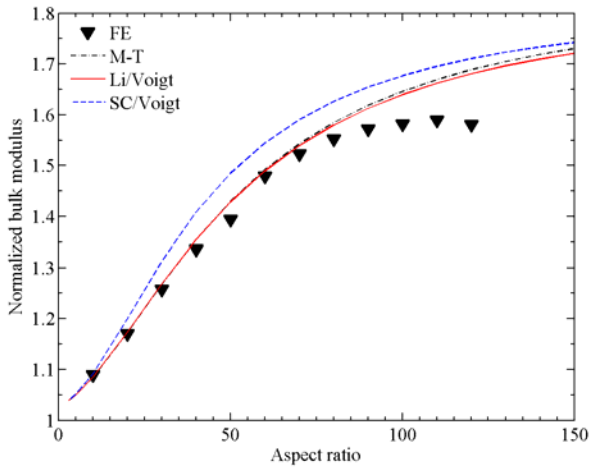

Fig.4. Normalized bulk modulus of ROFRC at 2% volume fraction and contrast of properties of 300 as a function of the fibers aspect ratio.

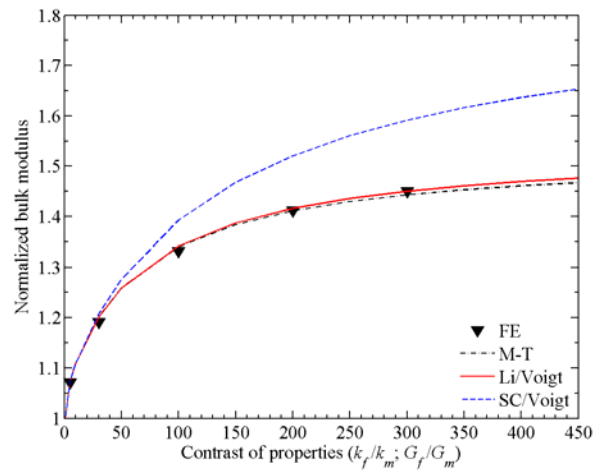

Fig.6. Normalized bulk modulus of ROFRCs with fibers of aspect ratio 20 as a function of the properties contrast at a volume fraction of 5%.

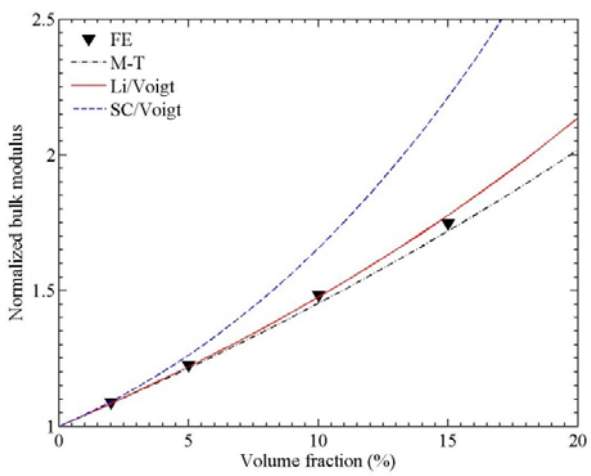

Fig.5. Normalized bulk modulus of ROFRCs with fibers of aspect ratio 10 as a function of the fibers volume fraction for a contrast of 300.

References

[1] B. Sadasivam, J. G. Cherng and P. K. Mallick, "Dynamic Response of Impact Damaged Random Fiber Automotive Composites," *Journal of Reinforced Plastics and Composites,* vol. 19, pp. 124-136, 2000.

[2] J. M. Corum, R. L. Battiste, M. B. Ruggles and W. Ren, "Durability-based design criteria for a chopped-glass-fiber automotive structural composite," *Composites Science and Technology,* vol. 61, pp. 1083-1095, 2001.

[3] Y. Hua and L. Gu, "Prediction of the thermomechanical behavior of particle-reinforced metal matrix composites," *Composites Part B: Engineering,* vol. 45, pp. 1464-1470, 2013.

[4] T. Mori and K. Tanaka, "Average stress in matrix and average elastic energy of materials with misfitting inclusions," *Acta Metallurgica,* vol. 21, pp. 571-4, 1973.

[5] B. Mortazavi, M. Baniassadi, J. Bardon and S. Ahzi, "Modeling of two-phase random composite materials by finite element, Mori–Tanaka and strong contrast methods," *Composites Part B: Engineering,* vol. 45, pp. 1117-1125, 2013.

[6] J. Segurado and J. Llorca, "A numerical approximation to the elastic properties of sphere-reinforced composites," *Journal of the Mechanics and Physics of Solids,* vol. 50, pp. 2107-2121, 2002.

[7] E. Ghossein and M. Levesque, "A fully automated numerical tool for a comprehensive validation of homogenization models and its application to spherical particles reinforced composites," *International Journal of Solids and Structures,* vol. 49, pp. 1387-1398, 2012.

[8] C. L. Tucker Iii and E. Liang, "Stiffness predictions for unidirectional short-fiber composites: Review and evaluation," *Composites Science and Technology,* vol. 59, pp. 655-671, 1999.

[9] S. Kari, H. Berger and U. Gabbert, "Numerical evaluation of effective material properties of randomly distributed short cylindrical fibre composites," *Computational Materials Science,* vol. 39, pp. 198-204, 2007.

[10] O. Pierard, C. Friebel and I. Doghri, "Mean-field homogenization of multi-phase thermo-elastic composites: a general framework and its validation," *Composites Science and Technology,* vol. 64, pp. 1587-1603, 2004.

[11] Y. Benveniste, "New approach to the application of Mori-Tanka's theory in composite materials," *Mechanics of Materials,* vol. 6, pp. 147-157, 1987.

[12] J. D. Eshelby, "The Determination of the Elastic Field of an Ellipsoidal Inclusion, and Related Problems," *Proceedings of the Royal Society of London. Series A. Mathematical and Physical Sciences,* vol. 241, pp. 376-396, August 20, 1957 1957.

[13] H. Moussaddy, D. Therriault and M. Levesque, "Assessment of existing and introduction of a new and robust efficient definition of the representative volume element," *Submitted to IJSS,* 2013.

[14] R. B. Barello and M. Levesque, "Comparison between the relaxation spectra obtained from homogenization models and finite elements simulation for the same composite," *International Journal of Solids and Structures,* vol. 45, pp. 850-867, 2008.

[15] T. Kanit, S. Forest, I. Galliet, V. Mounoury and D. Jeulin, "Determination of the size of the representative volume element for random composites: Statistical and numerical approach," *International Journal of Solids and Structures,* vol. 40, pp. 3647-3679, 2003.